Published August 30, 2004

CORRECTION

The Journal of General Physiology

Hui Zou, Lawrence M. Lifshitz, Richard A. Tuft, Kevin E. Fogarty, and Joshua J. Singer
Volume 124, No. 3, September 2004. Pages 259–272.

On further examination of the data obtained from the three-dimensional reconstructions we realized that in the two places where we took the data as being derived from a single channel there was more than one channel present. Although the conclusions reached from the data would not be altered, we want to inform the readers of this error.

For the data shown in Fig. 2 on page 265, although only one fluorescence transient was detected, there was a second caffeine-activated channel that opened before and closed after the fluorescence transient. Any fluorescence increase due to Ca influx through that channel was out of the image field and, therefore, would not contribute to the fluorescence measurements obtained for the figure. However, the brief closures in the current trace could have come from either channel. When constructing the figure, we had assumed all of the brief closures were from the channel of interest. To estimate how much of an error this assumption would produce, we recalculated the slope of ΔF_{total} (or signal mass) versus charge (ΔQ) assuming the opposite situation (all of the brief closures being from the other channel). The average difference in the slopes for all six planes remained nearly the same ($-1.8 \pm 0.7\%$ versus $-1.3 \pm 0.7\%$ for original versus recalculated data, respectively). The latter value is the same as that indicated in the original text by plotting ΔF_{total} versus time instead of charge. Therefore, the brief closures did not contribute significantly to the differences among the slopes of ΔF_{total} versus ΔQ as viewed from each optical plane.

The stretch-activated channel current (referred to at the top of the second column on page 266), recorded in a cell-attached patch, could have been derived from more than one channel. However, unlike for the caffeine-activated channels, the opening of more than one channel in the cell-attached patch would not have altered the slope of ΔF_{total} versus ΔQ because both measurements were obtained from the same patch with the channels essentially in the same plane. Also, there was essentially the same average difference in the slopes of ΔF_{total} versus ΔQ or versus time ($-4.5 \pm 4.9\%$ and $-3.3 \pm 5\%$, respectively). Both values were also in the original text.

We regret we did not catch these before the publication of the paper and hence did not include the above in the published analysis. However, none of what we have described above would have changed the conclusions based on this data.

Published August 30, 2004

Using Total Fluorescence Increase (Signal Mass) to Determine the Ca^{2+} Current Underlying Localized Ca^{2+} Events

Hui Zou,[1] Lawrence M. Lifshitz,[1,2] Richard A. Tuft,[1,2] Kevin E. Fogarty,[1,2] and Joshua J. Singer[1]

[1]Department of Physiology and [2]Biomedical Imaging Group, University of Massachusetts Medical School, Worcester, MA 01655

ABSTRACT The feasibility of determining localized Ca^{2+} influx using only wide-field fluorescence images was explored by imaging (using fluo-3) single channel Ca^{2+} fluorescence transients (SCCaFTs), due to Ca^{2+} entry through single openings of Ca^{2+}-permeable ion channels, while recording unitary channel currents. Since the image obtained with wide-field optics is an integration of both in-focus and out-of-focus light, the total fluorescence increase (ΔF_{total} or "signal mass") associated with a SCCaFT can be measured directly from the image by adding together the fluorescence increase due to Ca^{2+} influx in all of the pixels. The assumptions necessary for obtaining the signal mass from confocal linescan images are not required. Two- and three-dimensional imaging was used to show that ΔF_{total} is essentially independent of the position of the channel with respect to the focal plane of the microscope. The relationship between Ca^{2+} influx and ΔF_{total} was obtained using SCCaFTs from plasma membrane caffeine-activated cation channels when Ca^{2+} was the only charge carrier of the inward current. This relationship was found to be linear, with the value of the slope (or converting factor) affected by the particular imaging system set-up, the experimental conditions, and the properties of the fluorescent indicator, including its binding capacity with respect to other cellular buffers. The converting factor was used to estimate the Ca^{2+} current passing through caffeine-activated channels in near physiological saline and to estimate the endogenous buffer binding capacity. In addition, it allowed a more accurate estimate of the Ca^{2+} current underlying Ca^{2+} sparks resulting from Ca^{2+} release from intracellular stores via ryanodine receptors in the same preparation.

KEY WORDS: single channels • calcium imaging • SCCaFT • buffer binding capacity • smooth muscle

INTRODUCTION

Calcium ions play an important role in cell function, acting as effectors and/or signaling molecules for a variety of cellular biochemical and physiological processes. The development of a variety of Ca^{2+}-sensitive fluorescent indicators and advancements in imaging technology have enhanced the ability to follow both global and localized changes in intracellular Ca^{2+} at ever improving temporal and spatial resolution. Ratiometric Ca^{2+} indicators like fura-2 permit the measurement of intracellular Ca^{2+} concentration (Grynkiewicz et al., 1985). But, they tend to have a limited dynamic range and a significant fluorescence background, which reduce their sensitivity to small local increases in Ca^{2+}. On the other hand, certain nonratiometric Ca^{2+} indicators, such as fluo-3, although not able to give a dynamic direct read-out of the Ca^{2+} concentration, have very low fluorescence when not bound to Ca^{2+} and have a significant increase in fluorescence intensity upon binding Ca^{2+} (e.g., ~200 times for fluo-3; Harkins et al., 1993). Therefore, they can be especially useful for following small, local changes in Ca^{2+} inside the cell.

Fluo-3 and other such Ca^{2+} indicators have been employed to record localized Ca^{2+} fluorescence transients such as "Ca^{2+} sparks" and "Ca^{2+} puffs" due to Ca^{2+} release from intracellular stores through ryanodine receptors or IP3 receptors, respectively (Parker and Yao, 1991; Cheng et al., 1993; Lopez-Lopez et al., 1995; Nelson et al., 1995; Klein et al., 1996; Bootman et al., 1997; Koizumi et al., 1999). In addition, Ca^{2+} fluorescence transients due to Ca^{2+} influx through a single opening of plasma membrane caffeine-activated channels (Zou et al., 1999), and later, L-type Ca^{2+} channels (Wang et al., 2001) and stretch-activated channels (Zou et al., 2002), have also been recorded using these indicators.

One goal of these types of studies is to relate the observed localized fluorescence transients to the underlying Ca^{2+} currents. This would make it possible to obtain the Ca^{2+} current passing through plasma membrane nonselective cation channels in physiological saline or underlying Ca^{2+} sparks and puffs. However, specialized methods are required to obtain this relationship with nonratiometric Ca^{2+} indicators. For a brief overview of some of these methods see Zou et al. (2004).

The online version of this article includes supplemental material.

Address correspondence to Hui Zou, Dept. of Physiology, University of Massachusetts Medical School, 55 Lake Ave. North, Worcester, MA 01655. Fax: 508-856-5997; email: imaging.ionchannels@umassmed.edu

Abbreviations used in this paper: 3D, three-dimensional; fC, femtoCoulomb; PSF, point spread function; SCCaFT, single channel Ca^{2+} fluorescence transient.

J. Gen. Physiol. © The Rockefeller University Press • 0022-1295/2004/09/259/14 $8.00
Volume 124 September 2004 259–272
http://www.jgp.org/cgi/doi/10.1085/jgp.200409066

Published August 30, 2004

Sun et al. (1998) first introduced the insightful "signal mass" concept into fluorescence measurements of the Ca^{2+} flux underlying local Ca^{2+} events using confocal microscopy. They suggested that integrating the one-dimensional confocal linescan fluorescence signal, $\Delta F/F$, over three dimensions would provide the signal mass due to the Ca^{2+} flux associated with Ca^{2+} puffs. The rate of rise of the signal mass, therefore, could provide an estimate of the Ca^{2+} current generating the fluorescence increase; and the peak, an estimate of the total Ca^{2+} flux (neglecting Ca^{2+} removal mechanisms, which are on a much slower time scale). However, to ensure the accuracy of this method requires (a) that the Ca^{2+} fluorescence event be in sharp focus and the scanning line pass through its center, (b) that the fluorescence profile be spatially symmetrical, which may not be the case (for examples, see Shen et al., 2004; Figs. 2 and 7 in Wellman and Nelson, 2003, and Chandler et al., 2003), and (c) that the event be separated spatially from other fluorescence events.

Following its first use by Sun et al. (1998), the idea of using signal mass measurements has been adopted by a number of investigators, using confocal microscopy, to obtain measurements of the Ca^{2+} current underlying Ca^{2+} fluorescence events and/or the number of ryanodine receptors involved in such events or to compare fluorescence events in different preparations (Gonzalez et al., 2000; Hollingworth et al., 2001; Wang et al., 2001; Chandler et al., 2003; Zhou et al., 2003). However, calculating signal mass directly from linescan images could involve significant errors even if all of the assumptions mentioned above were met. This is because the signal-to-noise ratio decreases farther away from the Ca^{2+} influx site and the contribution of the noisier signal to the signal mass gets amplified due to the weighting based on the distance from the influx site (Sun et al., 1998; Rios and Brum, 2002). In an attempt to solve this problem, alternative methods have been developed for calculating the signal mass using the full spatial width at half maximum amplitude of the $\Delta F/F$ signal (Shirokova et al., 1999; Hollingworth et al., 2001; Chandler et al., 2003).

Confocal microscopy is used for most studies of localized Ca^{2+} fluorescence events because of its small depth of field, which minimizes the collection of out-of-focus light. However, for the application of the signal mass method, there are theoretical advantages provided by wide-field microscopy, because the wide-field microscope will collect light from not only the in-focus plane but also the out-of-focus planes. Therefore, a wide-field image itself should be an integration of the fluorescence along the optical axis. At each point in time, the fluorescence signal mass could be obtained in a straightforward manner by adding together the fluorescence increase due to Ca^{2+} influx in all of the pixels (Zou et al., 1999; Fogarty et al., 2000; ZhuGe et al., 2000; Zou et al., 2002). As a result, the first two requirements that apply to confocal microscopy should not be necessary for wide-field imaging. Computer simulations have been used to show that the signal mass obtained this way should provide a good measure of the underlying current whether or not the fluorescence event is in focus (Zou et al., 1999; ZhuGe et al., 2000). However, there has not been a systematic experimental establishment of this point (Zou et al., 2004).

The present study was performed (a) to experimentally determine the validity of using signal mass or ΔF_{total} measurements with wide-field microscopy for obtaining Ca^{2+} currents, especially to demonstrate that measurements of ΔF_{total} are independent of the focal plane, and (b) to use the method to determine the Ca^{2+} current when it cannot be measured directly. In addition, some of the characteristics of fluo-3 and endogenous buffers are explored. For this purpose, we have mainly used the properties of an 80-pS, plasma membrane, Ca^{2+}-permeable, nonselective cation channel that appears to be directly activated by caffeine (Guerrero et al., 1994a,b). The open time of the channel can be long and the channel density is low, possibly 10–15 channels per cell (scattered over the cell surface; Zou et al., 1999). These characteristics make it possible to record the unitary currents in the whole-cell recording configuration of the patch clamp. Also, as we have shown previously (Zou et al., 1999) with physiological concentrations of Ca^{2+} in the extracellular fluid, it is possible to record the fluorescence transient associated with Ca^{2+} entering the cell during a single opening of this channel (single channel Ca^{2+} fluorescence transient [SCCaFT]). All of the properties of this channel, especially those that enable simultaneous recording of the SCCaFT and the unitary current (without the membrane deformation associated with cell-attached patches as would be required with Ca^{2+} channels), make it a good choice for our present study.

MATERIALS AND METHODS

Single Smooth Muscle Cell Preparation

Smooth muscle cells were enzymatically dispersed from the stomach of the toad *Bufo marinus* as previously described (Fay et al., 1982; Lassignal et al., 1986) and used on the same day. All experiments were performed at room temperature.

Patch-clamp Recordings and Data Processing

The currents passing through caffeine-activated channels and stretch-activated channels were recorded with an Axopatch-1D amplifier (Axon Instruments, Inc.) using the whole-cell and cell-attached patch configurations, respectively. Currents were low-pass filtered at 200 Hz and sampled at 1 kHz. Brief transitions to the closed or open state could be masked by the filtering. Therefore, what we refer to as channel open time may correspond to a channel burst time. Sometimes a digitally generated 60-Hz signal

Published August 30, 2004

was subtracted to reduce the background noise. Caffeine-activated channels were opened by applying caffeine to the cell by pressure ejection from a glass pipette using a picospritzer (General Valve Corp.), and stretch-activated channels were opened by applying suction to the patch pipette (Zou et al., 1999, 2002).

Single discrete channel openings (or short bursts) were usually selected for the measurements described below. Total charge entry during channel openings was obtained by integrating the unitary channel current over time.

Wide-Field Digital Imaging and Fluorescence Measurements

Two-dimensional Imaging. Methods for two-dimensional (2D) Ca^{2+} fluorescence imaging and data processing were similar to those used by Zou et al. (1999, 2002). Fluorescence images were acquired using a custom-built high-speed digital imaging microscope with fluo-3 as the Ca^{2+} indicator. The standard system setup was the same as that diagramed in ZhuGe et al. (1999) except that a different oil immersion objective lens (60× magnification with a numerical aperture of 1.4) was used. We generally focused at the middle of the cell. Each image was composed of 128 × 128 pixels, each usually 0.333 μm square. At each pixel, the fluorescence at rest (F_0) was subtracted from the fluorescence (F) for each image in the image set, and the difference was used to construct the images (ΔF[1] = $F - F_0$ or $\Delta F/F_0 = [F - F_0]/F_0$), which were then smoothed (with a 3 × 3 kernel approximating a Gaussian with $\sigma = 1$ pixel) before display.[2] The resting fluorescence, F_0, was usually obtained by averaging the fluorescence intensity of 10 consecutive images when there was no fluorescence transient. The pixel with the maximum fluorescence increase for the transient was taken as the location of the channel and its fluorescence time course plotted in the figures. Measurements of fluorescence are given in units of photons detected by the camera.

The outline of the cell in the fluorescence ratio images was determined by applying a fluorescence intensity threshold. Several image sets were generally obtained from the same cell. To facilitate capturing the desired transients/channel openings we usually used a circular image buffer protocol (Zou et al., 1999; software provided by K.D. Bellve, Biomedical Imaging Group, University of Massachusetts Medical School). The read-camera control signal (sampled at 1 kHz) was simultaneously recorded with the current to facilitate the temporal alignment of the fluorescence trace with the corresponding current trace.

Three-dimensional Imaging. Three-dimensional (3D) imaging was used to provide images at planes above, below, and at the location of the channel. The digital imaging microscope was equipped with a computer-controlled piezoelectric focus drive to move the microscope objective lens, thereby scanning the focal plane of the objective lens through the thickness of the cell (for a more complete description see Kirber et al., 2001). The lens was moved at a constant velocity of 0.5 μm/ms and images continuously acquired every 2 ms. There was a turnaround time of 2 ms at the top and 5 ms at the bottom when the lens stopped moving so as to change direction from upward to downward or vice versa (Fig. 2 B). The images acquired during the turnaround times were discarded. We used this protocol because the coupling of the objective lens (60× water immersion, NA = 1.2) to the coverslip through the water immersion medium prevented us from moving the objective lens quickly enough in steps. We obtained a set of six images from six 1-μm-thick planes on average every 15.5 ms. The displayed $\Delta F/F_0$ images were obtained by deconvolution to remove the out-of-focus light (Fig. 2 A) from the stacks of optical images using the image restoration algorithm developed by members of the Biomedical Imaging Group (Carrington and Fogarty, 1987; Carrington et al., 1995). This algorithm takes into account the additional blurring resulting from the movement of the objective lens during image acquisition (see Kirber et al., 2001).

Determining the Ca^{2+} Current from the Total Fluorescence Change (ΔF_{total}) or Fluorescence Signal Mass

Signal mass measurements were obtained from an image area that was large enough to cover the entire fluorescence increase as determined from the ΔF or $\Delta F/F_0$ images (e.g., an area within a box like that shown in Fig. 1 A). Total fluorescence was measured from the raw images (not the $\Delta F/F_0$ images) by summing the fluo-3 fluorescence from all the pixels. To estimate Ca^{2+} entry into the cytoplasm, the change in total fluorescence (ΔF_{total}) was determined by subtracting the total fluorescence before the channel opened from the total fluorescence at each time point during the opening. The charge influx (ΔQ) was calculated by integrating current during the channel opening. When there was a global background fluorescence change (e.g., due to photobleaching), a linear extrapolation obtained from the baseline change before the transient was used to correct for background changes during the transient.

When Ca^{2+} enters into the cytoplasm, due to either release from intracellular Ca^{2+} stores or influx from the extracellular fluid, it will either remain free or it will bind to endogenous cellular buffers or fluorescent indicators like fluo-3. During a channel opening, ΔF_{total} can be taken as an estimate of the amount of Ca^{2+} that entered the cytoplasm and bound to fluo-3 at any time (Zou et al., 1999; Fogarty et al., 2000; ZhuGe et al., 2000; Zou et al., 2002). In addition, neglecting Ca^{2+} removal from the cytoplasm, ΔF_{total} will be, as shown below, linearly related to the Ca^{2+} influx (ΔCa^{2+}, the number of Ca ions entering the cytoplasm) over the same time period.

Determining the Relationship between ΔF_{total} and ΔCa^{2+}. From previous simulations, it was suggested that during the channel opening, at least for short time periods and for Ca^{2+} currents in the range of a few pA, there is a linear relationship between ΔF_{total} and ΔCa^{2+} (Zou et al., 1999; ZhuGe et al., 2000). If this is the case, then ΔF_{total}, in units of detected photons, and ΔCa^{2+} can be linked by a constant, k:

$$\Delta Ca^{2+} = k \cdot \Delta F_{total}. \quad (1)$$

The value of the constant, or converting factor, is affected by two components. The first is a fluorescence factor (f), which is

[1]To simplify the notation, all of the variables with a "Δ" prefix are time dependent except when denoted with "max" in the subscript.

[2]The construction of fluorescence images from either confocal or wide-field microscopy usually involves normalizing the fluorescence at each pixel to the resting fluorescence as $\Delta F/F_0$ or F/F_0. For wide-field fluorescence imaging of a macro fluorescence event occurring throughout the cell as would occur by activation of whole-cell Ca^{2+} current in a spherical or cylindrical cell, this procedure is appropriate in order to normalize for the effect of indicator concentration and/or cell depth. It might also be appropriate for confocal imaging of localized fluorescence events to normalize for the effect of indicator concentration where the fluorescence from each pixel is theoretically from a thin slice of the cell. However, the normalization of localized fluorescence events obtained with wide-field imaging can be misleading. This occurs because the same event (ΔF) occurring near the center of the spherical or cylindrical cell (the thicker part of the cell) would produce a smaller percent increase in fluorescence than at the edge (the thinner part of the cell) (Zou et al., 1999). Therefore, we chose to display most of our images without normalization by the resting fluorescence and used only the increase in fluorescence, ΔF, instead.

Published August 30, 2004

the measured fluorescence (in detected photons) per Ca^{2+}-bound fluo-3 molecule. The measured change in fluorescence will be related to the change in the amount of Ca^{2+}-bound fluo-3 molecules (ΔCaFluo-3) as follows:

$$\Delta F_{total} = f \cdot \Delta \text{CaFluo-3}. \quad (2)$$

The value of f results not only from the intrinsic properties of fluo-3 itself, but it is also a function of the image exposure time, laser excitation power, lens properties (e.g., magnification and numerical aperture), and other properties (e.g., camera, filters, mirrors, etc.) of the specific imaging system setup. Here, we have neglected the change in fluorescence due to the change in the amount of Ca^{2+}-free fluo-3 molecules ($<\sim 0.5\%$).

The second component is a buffer adjustment factor (f_b), which takes into account the amount of Ca^{2+} that binds to buffers other than fluo-3. Free Ca^{2+}, which is assumed to be small under our experimental conditions, is included in f_b for the analysis here. Therefore, f_b is equal to the number of Ca^{2+} ions that entered the cell (ΔCa^{2+}) for each Ca^{2+} ion that bound to fluo-3 such that

$$\Delta Ca^{2+} = f_b \cdot \Delta \text{CaFluo-3}. \quad (3)$$

The value of the buffer adjustment factor is dependent on the intracellular environment and the concentration of fluo-3.

It is straightforward to see from the above that k is simply the buffer adjustment factor divided by the fluorescence factor or

$$\Delta Ca^{2+} = k \cdot \Delta F_{total} = (f_b/f) \cdot \Delta F_{total}. \quad (4)$$

For the opening of a Ca^{2+}-permeable nonselective cation channel, the total charge entry over time (ΔQ), which is directly proportional to ΔCa^{2+} (provided that the Ca^{2+} current is a constant fraction of the total channel current), is obtained by integrating the channel current during the opening.

The converting factor, k, can be experimentally determined from the ΔF_{total} that occurs when a known amount of Ca^{2+} enters the cell. To do this, a 90 mM Ca^{2+} bathing solution (see below) was used so that all of the inward current was due to Ca^{2+} entry when a caffeine-activated channel opened. In this case, the number of Ca ions coming into the cell (ΔCa^{2+}) equals ΔQ divided by the charge of a Ca ion (3.2×10^{-19} C). With ΔF_{total} measured over the same period of time, from Eq. 1, we have $k = \Delta Q / (3.2 \times 10^{-19} \cdot \Delta F_{total})$. For these measurements, the values of ΔF_{total} and ΔQ were usually taken from the time just before the channel opened until just after the channel closed and therefore are denoted as $\Delta F_{total\text{-}max}$ and ΔQ_{max} (see Fig. 3). $\Delta F_{total\text{-}max}$ and ΔQ_{max} can be obtained with higher accuracy by averaging through the baseline and the near steady-state plateau and this method was used to obtain the converting factor and related results.

The value of k, through its dependence on f (Eq. 4) changes if the imaging system set-up is changed and is also affected by the image exposure time. All of the images involved in determining k and related measurements were obtained in "full-frame rate" mode where images were acquired every 10 ms with a 10-ms exposure time. To apply the value of k to measurements where the image exposure time is different, the value of the measured ΔF_{total} has to be normalized so that the effective exposure time is 10 ms. For example, if the k were to apply to the results shown in Fig. 1 (where images were acquired every 15 ms with a 6-ms exposure time), the value of ΔF_{total} would have to be multiplied by 10/6.

On the other hand, f_b is a function of the intracellular environment (particularly the concentration of fluo-3) and not the imaging system setup. Therefore, if we obtain the converting factor for one imaging system setup using a known Ca^{2+} current as described above and separately obtain a measure of f using the same set-up, we can then obtain the value of f_b. Moreover, if we should choose to use a different set-up, with the value of f_b known, we can calculate the new converting factor by merely obtaining f with this set-up. f_b can also be used to estimate the equivalent binding capacity of the endogenous buffers (see DISCUSSION). Therefore, it is useful to be able to obtain values for f and f_b.

Determining the Fluorescence Factor, f, for Ca^{2+}-bound Fluo-3 Molecules and the Buffer Adjustment Factor, f_b. When Ca^{2+} and fluo-3 are in equilibrium (as at rest):

$$[\text{CaFluo-3}] = [Ca^{2+}] \cdot [\text{Fluo-3}]_T / (K_d + [Ca^{2+}]). \quad (5)$$

Here, [CaFluo-3] is the Ca^{2+}-bound fluo-3 concentration, $[\text{Fluo-3}]_T$ is the total fluo-3 concentration, K_d is the dissociation constant for fluo-3 and Ca^{2+} (estimated to be 1.13 μM inside the cell; Smith et al., 1998), and $[Ca^{2+}]$ is the free Ca^{2+} concentration. Neglecting the fluorescence from Ca^{2+}-free fluo-3, from Eqs. 2 and 5:

$$f = F_{total}/\text{CaFluo-3} = F_{total}/(A_v \cdot V \cdot [\text{CaFluo-3}]) = F_{total} \cdot (K_d + [Ca^{2+}])/(A_v \cdot V \cdot [\text{Fluo-3}]_T \cdot [Ca^{2+}]) \quad (6)$$

F_{total} is the measured resting fluorescence in detected photons, A_v is Avogadro's number, and V is the volume containing the fluo-3 molecules from which the F_{total} measurement is obtained. When $[Ca^{2+}]$ is saturating, [CaFluo-3] essentially equals $[\text{Fluo-3}]_T$ and, therefore, Eq. 6 reduces to

$$f = F_{total}/(A_v \cdot V \cdot [\text{Fluo-3}]_T). \quad (6a)$$

Experimentally, f was obtained using rectangular glass capillary tubes with a light path length of 20 μm (Vitro Dynamics Inc.). They were filled with a physiological saline solution containing 2 mM Ca^{2+} and 1, 5, or 10 μM fluo-3 penta-potassium salt. The same imaging system setup used for the experiments with isolated cells was used, and F_{total} was usually measured from the central 100 × 100 pixels of the image field. The volume of the segment of the tube, from which the measurements were obtained, was the area of the central image field times the light path length of the tube. From this volume, the measured F_{total}, and the total concentration of fluo-3, we could obtain f from Eq. 6a. Because other configurations of the imaging system (with different objective lenses) were also used, f could be obtained for each configuration and will be detailed in the text where appropriate. The advantage of using the glass capillary tubes to determine f instead of an estimated segment of the cell volume (see ZhuGe et al., 2000) is that the value obtained using capillary tubes is independent of the estimates of the cell volume, the resting Ca^{2+} concentration, and the K_d. Values of f given in the text were normalized to a 10-ms exposure time. Once f and k have been obtained, the buffer adjustment factor, f_b, can be determined using Eq. 4.

Determining the Ca^{2+} Current Underlying a Fluorescence Transient. For a nonselective Ca^{2+}-permeable plasma membrane cation channel, integrating the current during the channel opening will provide ΔQ_{max}. With $\Delta Ca^{2+}{}_{max}$ obtained from $\Delta F_{total\text{-}max}$ using Eq. 1, the fraction of the current carried by Ca^{2+} is simply $3.2 \times 10^{-19} \cdot \Delta Ca^{2+}{}_{max}/\Delta Q_{max}$ or $3.2 \times 10^{-19} \cdot k \cdot \Delta F_{total\text{-}max}/\Delta Q_{max}$. The actual unitary Ca^{2+} current is determined by multiplying the total unitary channel current at the same membrane potential by this fraction.

Published August 30, 2004

Alternatively, the rate of rise for ΔCa^{2+} with time during the channel opening can be used to obtain the underlying Ca^{2+} current (i_{Ca}):

$$i_{Ca} = 3.2 \times 10^{-19} \cdot \Delta Ca^{2+}/\Delta t = 3.2 \times 10^{-19} \cdot k \cdot \Delta F_{total}/\Delta t. \quad (7)$$

This equation is especially useful for those fluorescence transients where the underlying current cannot be recorded and/or the duration of the channel openings is not known (like for Ca^{2+} sparks). But there are also limitations with this method (see DISCUSSION).

For measurements of the fraction of the current carried by Ca^{2+} through caffeine-activated channels, there was no significant difference in $\Delta F_{total\text{-}max}$ between the two groups of cells: one bathed in the 90 mM Ca^{2+} solution used to determine k and the other bathed in 1.8 mM Ca^{2+}.

Criteria for Data Selection for Analysis

For most of the fluorescence transients analyzed, it was necessary that (a) the transient of interest be separated in time and space from other transients; (b) ΔF_{total} measurements, though confined to a limited region of the cell, include all of the fluorescence signal associated with the transient within the field of view of the camera; (c) the transient not be so out of focus that it was hard to distinguish the transient from the noise, (d) the underlying channel opening be sufficiently long; and (e) for measuring charge influx, ΔQ, the channel current associated with the transient be free of interfering currents from other channel openings.

For two of the 3D transients where there were interfering currents, instead of plotting ΔF_{total} versus ΔQ, we plotted ΔF_{total} versus time. We could do this because there appeared to be no significant closures (i.e., the channel was essentially always open so ΔQ would increase linearly with time) judging from the in-focus ΔF, which clearly reflects the openings and closings of the channel (Zou et al., 1999; Video 1, available at http://www.jgp.org/cgi/content/full/jgp.200409066/DC1). Statistical data are expressed as the mean ± SEM.

Obtaining the Point Spread Function (PSF) of the Microscope

To help compare the results here using our custom-built microscope with what might be obtained using other (commercially available) microscopes (see DISCUSSION), the microscope PSFs were obtained using fluorescent microspheres (PS-Speck Microscope Point Source Kit). The microspheres (0.175 μm) were diluted in 90% glycerol mounting medium, applied to a No. 1.5 glass coverslip, and sealed onto a glass slide. Only isolated, individual beads lying on the coverslip surface were used. Images were acquired as optical sections by moving the objective lens over a range of ±10 μm from the microsphere.

Solutions

The bathing solution used for the experiments described here usually contained (in mM) NaCl 130, KCl 3, $CaCl_2$ 1.8, $MgCl_2$ 1, and Hepes 10 (pH adjusted to 7.4 using NaOH). The usual whole-cell pipette solution contained (in mM) KCl 137, $MgCl_2$ 3, Hepes 10, Na_2ATP 3, and fluo-3 pentapotassium salt 0.05 (pH adjusted to 7.2 using KOH). At times we also used a bath solution that contained (in mM) NaCl 127, KCl 3, $CaCl_2$ 1.9, $MgCl_2$ 1, and Hepes 10 (pH adjusted to 7.4 using NaOH); and a pipette solution that contained (in mM) KCl 130, $MgCl_2$ 1, Hepes 20, Na_2ATP 3, Na_3GTP 1, and fluo-3 pentapotassium salt 0.05 (pH adjusted to 7.2 using KOH). A high $[Ca^{2+}]$ bath solution, used for calibration purposes with caffeine-activated channels so that at negative potentials the only charge carrier of the inward current would be Ca^{2+}, contained (in mM) $CaCl_2$ 90 and Hepes 10 (pH adjusted to 7.4 using $Ca[OH]_2$). In the text, we designate the latter as the 90 mM Ca^{2+} solution.

For most of the experiments described here, we wished to remove any possible contributions from intracellular Ca^{2+} stores, therefore thapsigargin (1 μM) was added to the bathing solutions and ryanodine (100 μM) was included in the patch pipette solution. Caffeine (20 mM in the bathing solution) was also applied to the cells before the beginning of experiments using the Picospritzer. These treatments have been previously employed to successfully block effects from the intracellular stores (ZhuGe et al., 1999; Zou et al., 1999). The stock solutions for thapsigargin (10 mM) and ryanodine (100 mM) were in DMSO and stored at −20°C.

Online Supplemental Material

The online supplemental material (Fig. S1 and Video 1) are available at http://www.jgp.org/cgi/content/full/jgp.200409066/DC1. Fig. S1 shows the total fluorescence of a microsphere as a function of its distance from the focus point of the microscope (for both the microscope used in the present study and one that is commercially available). This figure demonstrates that our findings concerning the signal mass method would also be valid for other wide-field imaging systems (see Discussion). Video 1 shows the sensitivity of the in-focus SCCaFT to the openings and closings of the channel.

RESULTS

Total Fluorescence Increase, ΔF_{total}, Is Linearly Related to Charge Entry, ΔQ

When caffeine was applied to a toad stomach smooth muscle cell with the whole-cell membrane potential held at −80 mV, the inward unitary currents and the fluorescence increase associated with Ca^{2+} entering the cell were recorded simultaneously (Fig. 1, A and B). Temporal integration of the unitary current provided the time course of total charge entry (ΔQ) and spatial integration of the change in fluorescence at each pixel (ΔF) provided the time course of the increase in total fluorescence (ΔF_{total}) associated with the channel opening (Fig. 1 B). Except when channel closures occurred, ΔQ increased linearly with time, suggesting a constant Ca^{2+} influx. These closures also affect the time course of ΔF_{total}. However, even with the presence of brief closures, we found that there was a linear relationship between ΔF_{total} and ΔQ (and therefore ΔCa^{2+}) during a channel opening ($r^2 = 0.99$; Fig. 1 C). Therefore, the relationship between ΔF_{total} and ΔQ provides a better way of characterizing these events than the changes of ΔF_{total} with time. A linear relationship between ΔQ and ΔF_{total} was obtained from at least 31 transients in 16 cells with different solutions, suggesting that for our experimental conditions, the value of the converting factor (and therefore f_b) does not change over the time period of a channel opening.

ΔF_{total} Measurements Are Independent of the Focal Plane

Because the light detected using wide-field microscopy comes from both in- and out-of-focus planes, a 2D wide-

Published August 30, 2004

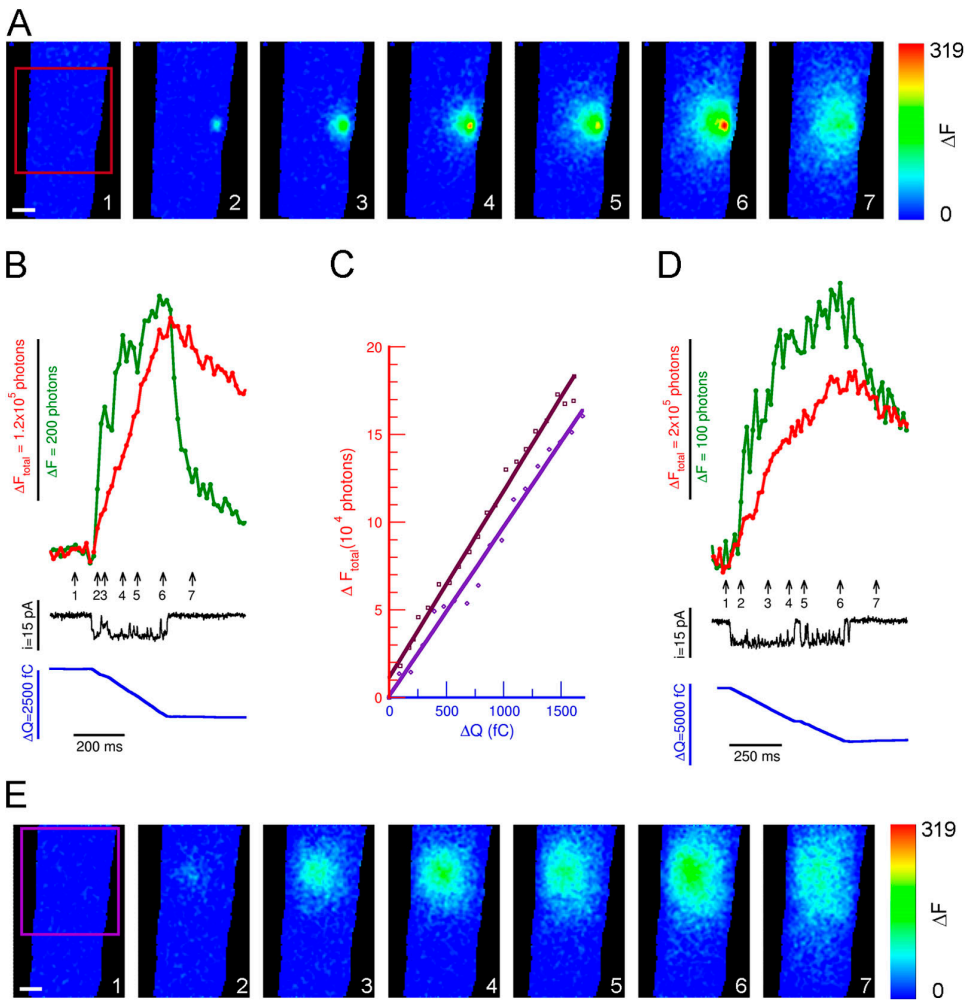

FIGURE 1. There is a linear relationship between Ca^{2+} influx and fluorescence "signal mass" (ΔF_{total}) that appears not to be affected by the relative position of the transient to the focal plane of the wide-field microscope. An in-focus transient and an out-of-focus transient were detected from the same cell. A series of seven sequential images, starting from the one preceding the channel opening, are displayed for each transient (A for the in-focus and E for the out-of-focus transients). The images were obtained at the time points indicated by the correspondingly numbered arrows in B and D, respectively. Shown in B and D are the measurements associated with the transients: the local fluorescence increase at the channel (ΔF, green trace), the total fluorescence increase (ΔF_{total}, red trace) within the color coded boxes, the unitary current record (i, black trace), and the integration of the current (ΔQ, blue trace). During the channel opening, the relationship between ΔQ and ΔF_{total} can be fitted by a straight line for both the in-focus transient ($r^2 = 0.99$, maroon colored trace, C) and the out-of-focus transient ($r^2 = 0.99$, indigo colored trace). The slopes are 114 vs. 100 detected photons per femtoCoulomb, respectively. This suggests that there is also a linear relationship between ΔCa and ΔF_{total}. For the in-focus transient (B), ΔF_{total} increases nearly linearly with time during the channel opening. However, for the out-of-focus transient (D), the rate of rise of ΔF_{total} declines after ~200 ms. From a plot of ΔF_{total} versus charge influx over the entire opening, it was determined that most of the decline (~2/3) is due to the fluorescence from Ca^{2+}-bound fluo-3 extending beyond the measured region and the rest, an increasing number of fast closures. For better visualization of the transients, ΔF images are shown here instead of the raw images from which ΔF_{total} was obtained. The areas used to obtain the signal mass measurements are indicated in the left-most images. Images were obtained every 15 ms with an exposure time of 6 ms. Bars, 5 μm. This set of whole-cell recordings from the caffeine-activated channel was obtained with the pipette solution containing (in mM) KCl 130, $MgCl_2$ 1, Hepes 20, Na_2ATP 3, Na_3GTP 1, and fluo-3 pentapotassium salt 0.05 (pH = 7.2); and the bath solution containing (in mM) NaCl 127, KCl 3, $CaCl_2$ 1.9, $MgCl_2$ 1, and Hepes 10 (pH = 7.4).

field image is actually an integration of light throughout the depth of the cell. Therefore, theoretically, for the same Ca^{2+} influx, ΔF_{total} should not change regardless of the location of the channel relative to the plane of focus. For example, if the transient in Fig. 1 A was not in focus, we still would have expected the relationship between the ΔF_{total} and ΔQ to be the same. Although this could be predicted from computer simulations (Zou et al., 1999; ZhuGe et al., 2000), we performed two sets of experiments to determine if this was indeed the case.

In the first set of experiments, we obtained different SCCaFTs in the same cell that were either in or out of focus depending on their location. For some other cells, recordings of in- and out-of-focus SCCaFTs were obtained with the objective lens moved to different positions along its optical axis. Therefore, SCCaFTs from the same location could be recorded either close to or farther away from the focal plane. An example is shown in Fig. 1 (B and D) with a pair of SCCaFTs recorded from the same cell, one from its punctate appearance being in focus (Fig. 1 A) and the other from its diffuse appearance, out of focus (Fig. 1 E). A plot of ΔF_{total} versus ΔQ showed nearly the same slope for both transients (Fig. 1 C). For the cell in Fig. 1, we obtained three in-focus transients from the same location (as

Published August 30, 2004

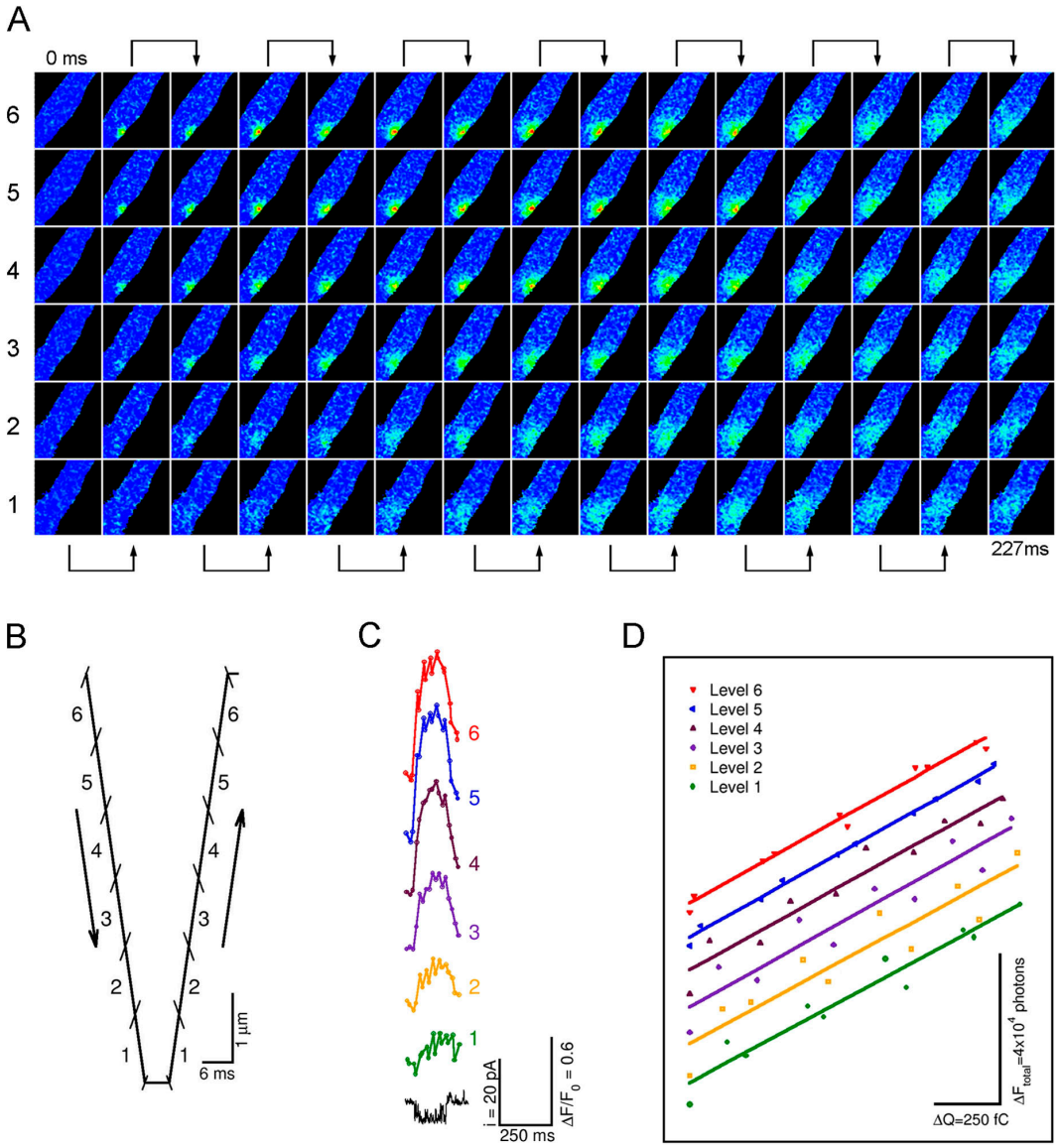

FIGURE 2. Continuous 3D imaging shows a similar relationship between ΔF_{total} and ΔQ from images of a SCCaFT in different focal planes. A SCCaFT was detected using a continuous 3D imaging technique. Restored $\Delta F/F_0$ images are shown at different focal planes during the 227 ms from before the channel opened until after the channel closed (A). The 3D restoration was performed using the point spread function acquired by imaging a fluorescent bead with the same protocol. The first image in the sequence is at the top left, acquired near the top of the cell. The image acquisition sequence then runs down the first column (toward the bottom of the cell) and back up the second column and so on, as indicated by the arrows above and below the images with the last image at the bottom right. The channel appears to be located within the top two slices. At an image pixel size of 300 nm square, 3D imaging was accomplished by continuously scanning the focus of the objective lens through the cell. A schematic drawing of the time course of the position of the objective lens is shown in B. Fluorescence images were continuously acquired over a 6-µm depth of the cell as the objective moved at a constant velocity of 0.5 µm/ms. With a 2-ms exposure time, each image represents a 1-µm-thick slice of the cell. The time course of fluorescence changes ($\Delta F/F_0$) from the restored images at each plane, measured in a 1.5-µm square box overlaying the transient, were plotted above the current trace (C). ΔF_{total} was obtained from the unrestored images at each plane and is plotted versus the total charge accumulated due to the channel opening at the time each image was acquired (D). The slopes of the least squared fits to ΔF_{total} versus ΔQ at each level are nearly the same being on average within 1.8% of that of the most in-focus plane (level 5). The slopes (in detected photons/fC) and r^2 values for levels 1–6, respectively, are 37.4, 0.94; 37.7, 0.87; 38.8, 0.90; 38.5, 0.94; 39.0, 0.99; and 38.8, 0.99. The ΔF_{total} plots for each level were shifted vertically to avoid overlapping. Because of a small amount of hysteresis associated with lens movement, ΔF_{total} during the upward excursion is slightly different from that during the downward excursion. Bath and pipette solutions are the same as for Fig. 1.

shown in Fig. 1 A), one out-of-focus transient from a location close to that of the in-focus transients, and two out-of-focus transients from a third location (as shown in Fig. 1 E). The slopes from plots of ΔF_{total} versus ΔQ (for approximately the first 200 ms) of the three in-focus transients were close with values of 114, 93, and

Published August 30, 2004

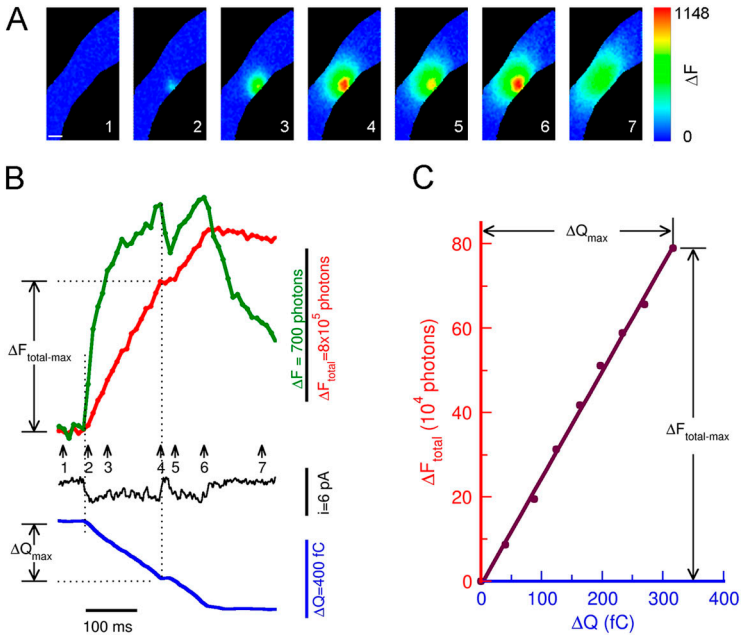

FIGURE 3. Obtaining the converting factor between ΔF_{total} and Ca^{2+} influx using a known Ca^{2+} current. (A) Selected images obtained at the times indicated by the correspondingly numbered arrows in B. (B) Local fluorescence increase (ΔF) at the channel (green trace), ΔF_{total} (red trace), the Ca^{2+} current (black trace), and ΔQ (due solely to Ca^{2+} entry, blue trace) with time associated with the opening of the caffeine-activated channel. The relationship between the total fluorescence increase and total Ca^{2+} entry, shown for the channel opening defined between the two vertical lines in B, can be fitted by a straight line ($r^2 = 0.99$, C). Indicated in B and C are measurements of $\Delta F_{total\text{-}max}$ and ΔQ_{max}, the values of the total increase in ΔF_{total} and ΔQ, respectively, from the time before the channel first opened to the time at the first long closure. The images were acquired every 10 ms with a 10-ms exposure time. Bar, 5 μm. The 90 mM Ca^{2+} bath solution and the usual pipette solution were used.

100 (or 102 ± 6) detected photons per femtoCoulomb (fC). The slopes of the three out-of-focus transients shared similar values of 96, 100, and 78 (or 91 ± 7) detected photons per fC. 13 additional transients were obtained from 4 other cells. When comparing the slopes of the more out-of-focus transients with that of the most in-focus transient in the same cell (as in Fig. 1 C), the difference on average for 12 pairs was 7.6 ± 5.5%. In general it appears that for the same charge influx, the measured total fluorescence change, ΔF_{total}, is independent of the focal plane (within certain limitations, see below and DISCUSSION).

In the second set of experiments, the same Ca^{2+} transient was measured from six different focal planes, taking advantage of the fast 3D imaging capability of our imaging system. As shown in Fig. 2 A, the SCCaFT appeared to be located close to planes 5 and 6 (where it was most punctate in appearance). It was most out of focus in plane 1 based on its extremely diffuse appearance. From the in-focus planes, the fluorescence change ($\Delta F/F$) in the vicinity of the channel is much greater with a more rapid rise and fall and with a steeper spatial gradient than for those planes that are more out of focus (Fig. 2 C). However, the slopes for the linear relationship between ΔF_{total}, obtained from the unrestored images, and ΔQ are essentially the same for all of the six planes (Fig. 2 D). When obtained from the more out-of-focus planes, the slopes differed by −1.8 ± 0.7% compared with that from the most in-focus plane (as in Fig. 1 C). The fact that the slopes of the six linearly fitted curves are essentially the same demonstrates that the same Ca^{2+} current can be determined based on ΔF_{total} (fluorescence signal mass) measurements from both in- and out-of-focus wide-field images. A similar result was obtained from a stretch-activated channel current in another cell where the difference of the slopes was −4.5 ± 4.9%.

There were other 3D experiments where we were able to obtain the fluorescence transient in all six planes, but because there were interfering openings in the current trace, we could not obtain the charge influx underlying the transient. Two of these transients were judged to be free of long closures using the technique described near the end of MATERIALS AND METHODS. Since the same Ca^{2+} current underlies the fluorescence changes in all of the planes, we would expect the same ΔF_{total} in each plane. We compared ΔF_{total} versus time, instead of charge influx, for the out-of-focus planes with that of the most in-focus plane for these two transients. The difference in slopes was 10.3 ± 2.0% and −4.7 ± 5.2%. Application of this analysis to the two transients described in the previous paragraph resulted in the difference in slopes of −1.3 ± 0.7% and −3.3 ± 5.0%.

In summary, it appears that ΔF_{total} is directly related to the underlying Ca^{2+} current; and therefore the Ca^{2+} current can be determined using wide-field microscopy even if the channel is not in the focal plane of the 2D image. To do this requires obtaining the converting factor between ΔF_{total} and ΔCa^{2+}.

Determining the Converting Factor (k), the Fluorescence Factor (f), and the Buffer Adjustment Factor (f_b)

The converting factor between ΔF_{total} and ΔCa^{2+} can be determined using the 90 mM Ca^{2+} bath solution such that Ca^{2+} is the only ion available to carry the inward current (Fig. 3). There was a linear relationship between ΔF_{total} and ΔQ during the time of the channel opening (Fig. 3 C). With Ca^{2+} being the only charge

Published August 30, 2004

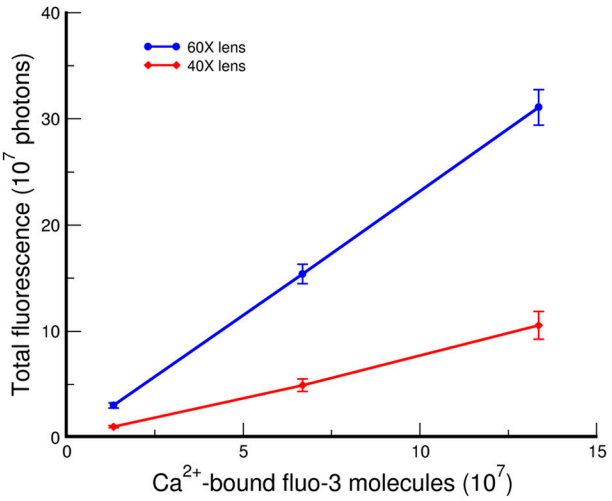

FIGURE 4. Determination of the fluorescence factor, *f*, for Ca^{2+}-bound fluo-3 molecules. The fluorescence emission is linearly related ($r^2 = 1.0$) to the number of Ca^{2+}-bound fluo-3 molecules. Measurements were obtained from a 100 × 100 pixel area from rectangular glass capillary tubes. For the 60× magnification objective lens (NA = 1.4, used for most of the experiments), *f*, determined by the slope (Eq. 6a), is 2.34 detected photons per Ca^{2+}-bound fluo-3 molecule. Each point is the mean ± SEM for seven or eight sets of glass capillary tubes. For the 40× magnification objective lens (NA = 1.3), measurements were taken with three sets of glass capillary tubes, yielding a slope of 0.8 detected photons per Ca^{2+}-bound fluo-3 molecule ($r^2 = 0.998$). For measurements for both lenses, the value at each point was usually taken from the average of a number of recordings at 2- and 4-ms exposure times. The pixel size was 0.333 μm; and the light path length, 20 μm. The slopes were normalized for a 10-ms exposure time.

carrier, the total charge entry, ΔQ_{max}, directly provides the number of Ca ions that entered the cell ($\Delta Ca^{2+}_{max} = \Delta Q_{max}/3.2 \times 10^{-19}$). The converting factor can be obtained from the ratio of ΔCa^{2+}_{max} to $\Delta F_{total\text{-}max}$. A linear relationship between ΔF_{total} and ΔQ was obtained for 10 transients in 7 cells, and the average ratio of ΔCa^{2+}_{max} to $\Delta F_{total\text{-}max}$ for these transients provided a converting factor of 1.65 ± 0.12 Ca^{2+} ions per detected photon for a 10-ms exposure time. These results were obtained at −80 mV to increase the size of the unitary current under whole-cell current recording conditions.

To determine *f*, fluorescence emission was obtained using capillary tubes containing 1, 5, and 10 μM fluo-3 concentrations in the presence of 2 mM (saturating) Ca^{2+} as described in MATERIALS AND METHODS. Measurements were obtained with an exposure time of 2 or 4 ms and normalized to a 10-ms time period. Using Eq. 6a and measurements with the standard setup, we found that *f* is equal to 2.34 detected photons per Ca^{2+}-bound fluo-3 molecule (Fig. 4).

With the values of *f* and *k* known, f_b can be determined from Eq. 4 and is equal to 3.86, i.e., on average 3.86 Ca^{2+} ions enter the cytoplasm for every Ca ion that binds to fluo-3. Therefore, ~26% (=1/3.86) of the Ca^{2+} that entered the cytoplasm binds to fluo-3 with the rest binding to endogenous buffers except for a very small amount of free Ca^{2+} (see DISCUSSION). A similar value was obtained by Chandler et al. (2003) from their computer simulations of Ca^{2+} sparks in frog skeletal muscle using 100 μM fluo-3, and it is a little less than one half of the value that can be derived from the release flux data of Rios et al. (1999) with an average estimated fluo-3 concentration of 260 μM.

Determining the Fraction of the Current Carried by Ca^{2+} and the Unitary Ca^{2+} Current for Nonselective Cation Channels

Using the converting factor obtained with the 90 mM Ca^{2+} solution, we determined the fraction of the current carried by Ca^{2+} for the caffeine-activated channel at −80 mV using the standard solutions with the extracellular solution containing physiological levels of Ca^{2+}. For 15 transients in 6 cells, there was a linear relationship between ΔF_{total} and ΔQ over the time of the channel opening (as in Fig. 1 C). ΔCa^{2+}_{max} can be obtained from the $\Delta F_{total\text{-}max}$ that accompanied a channel opening and the converting factor (Eq. 1). The fraction of the current carried by Ca^{2+} could then be calculated from $3.2 \times 10^{-19} \cdot \Delta Ca^{2+}_{max}/\Delta Q_{max}$. In this case ΔQ_{max}, the integral of the current during a channel opening, includes the current carried by other cations in addition to Ca^{2+}. To use the converting factor in this way requires that the same imaging system setup and pipette (intracellular) solution (including the concentration of fluo-3) be used for both groups of cells. For the 15 transients, the fraction of the inward current carried by Ca^{2+} is 20.2 ± 0.8%. This makes the Ca^{2+} current 1.4 pA for a 7.1-pA total inward unitary current at −80 mV. The value of 20.2% is close to that (18.9%) found by Guerrero et al. (1994b) using a different methodology and somewhat different solutions (but with the same extracellular Ca^{2+} concentration) and is in the upper range for other nonselective cation channels where Ca^{2+} fluxes were obtained (Neher, 1995; Burnashev, 1998; Ohyama et al., 2000; Zou et al., 2002).

Although the openings of caffeine-activated channels tend to be long, brief openings were also examined and included in the above result. The relationship between the fraction of current carried by Ca^{2+} and the value of the measured ΔF_{total} is independent of the duration of the channel opening (Fig. 5). Illustrated in Fig. 5 is an example of a very brief, spark-like SCCaFT recording with a channel opening lasting <12 ms. This SCCaFT resembles a Ca^{2+} spark in a number of characteristics: its rise time, percent change in fluorescence, $t_{1/2}$, and full width at half maximum (FWHM) are all in the range of those for a Ca^{2+} spark in the same cell type (ZhuGe et al., 2000). More importantly, its signal mass, when corrected for differences in *f* (see DISCUSSION), indicates a similar increase in the number of Ca^{2+}-bound

Published August 30, 2004

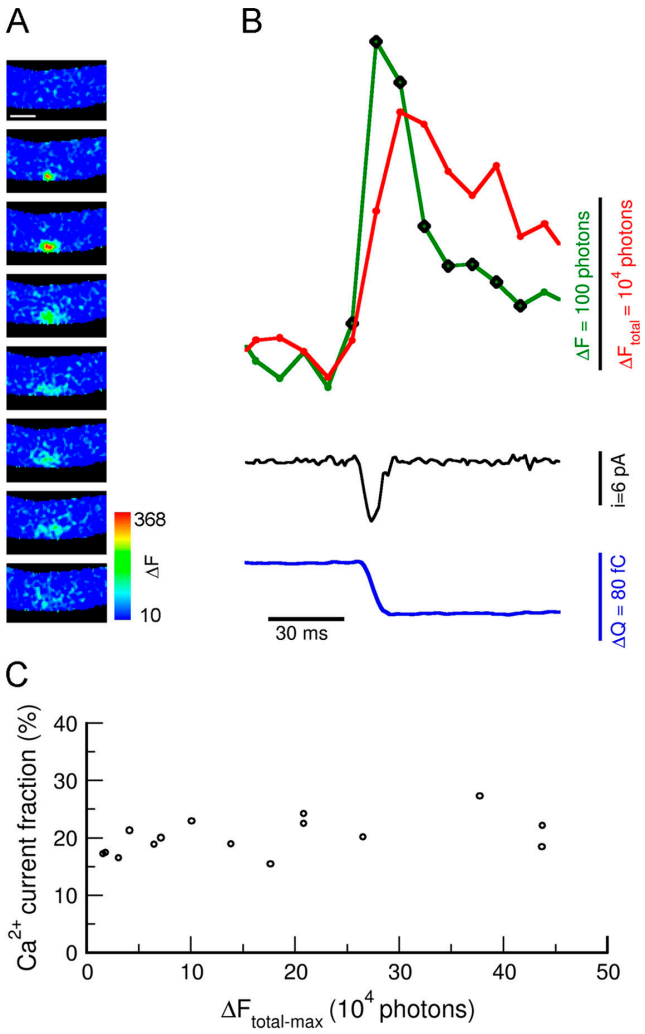

FIGURE 5. Total fluorescence increase is a valid measurement for Ca^{2+} entry independent of the duration of the underlying channel opening. A brief, spark-like, fluorescence transient was recorded with the underlying channel opening (or burst time) of ~12 ms. A series of consecutive images (starting from the one immediately preceding channel opening) is displayed from top to bottom (A). Both ΔF and ΔF_{total} are plotted in B against time. The diamond-shaped points in the ΔF trace indicate the time for the sequence of images in A. The rise time of ΔF was 10 ms, change in fluorescence was ~15%, $t_{1/2}$ of decay was <20 ms, and the full width at half maximum (FWHM) ~2 μm at the peak. Because of the filtering, the channel opening in the current trace appeared distorted, and the recorded peak unitary current of 6.8 pA is less than the average peak value of 7.1 pA. We can obtain an average current of at least 4 pA by dividing the total charge influx by the maximum channel open (or burst) time of 12 ms. Because on average 20.2% of the current is carried by Ca^{2+}, the average Ca^{2+} current passing through the channel is at least 0.81 pA, in the range of the average Ca^{2+} currents underlying sparks as estimated from the Ca^{2+} spark signal mass in DISCUSSION. For a group of 15 transients, there is no apparent relationship (C) between the value of the measured $\Delta F_{total-max}$ (dependent mainly on the channel open duration) and the fraction of current carried by Ca^{2+}. Standard bath and pipette solutions were used in these experiments. The images were acquired every 10 ms with a 10-ms exposure time. Bar, 5 μm.

fluo-3 molecules to that expected on average from a Ca^{2+} spark (~7,000 versus 10,000, respectively). Therefore, the converting factor obtained from the present study could also be applicable for determining Ca^{2+} current underlying sparks in these cells (see DISCUSSION).

DISCUSSION

The results shown in this study provide experimental evidence that Ca^{2+} flux through a single channel can be quantitatively measured using wide-field microscopy with single wavelength fluorescent indicators (e.g., fluo-3) by measuring total fluorescence increase (ΔF_{total}, or signal mass). With a known Ca^{2+} current for calibration, a converting factor between ΔF_{total} and the underlying Ca^{2+} influx was obtained as a characteristic of the cell and the imaging system. The converting factor could then be applied to obtain other Ca^{2+} currents (e.g., that normally pass through caffeine-activated channels or that underlie Ca^{2+} sparks) under the same experimental conditions. Furthermore, the endogenous buffer binding capacity can also be estimated from the calibrated fluorescence measurements (see below).

A wide-field imaging microscope collects light not only from the two dimensions of the focal plane but also above and below it. The illumination intensity and the collection angle are essentially unchanged, at least within the range of the cell thickness (a few micrometers). Therefore, the same fluorescence intensity and the same fraction of the entire fluorescence emission would be collected whether the transient is in or out of focus. However, an out-of-focus transient forms an enlarged image with less intensity at each pixel. This results in a decrease in signal-to-noise ratio not only for each pixel but also for ΔF_{total}. The latter occurs also because measurements have to be obtained from a larger image area in order to gather all the fluorescence from an out-of-focus transient. This decrease in overall signal-to-noise ratio may prevent the technique from being used for transients that are far out of focus. Nevertheless, this method should prove useful for channels within at least 4 μm of the focal plane, as determined from the 3D images (Fig. 2).

To determine if our findings here would also be valid for other wide-field imaging systems, we compared the total fluorescence measurements (background corrected) using our system with those of a commercially available digital imaging microscope. We did this by measuring the total fluorescence from images acquired for constructing the PSF of each microscope using a fluorescent microsphere. Each of the images was acquired with the microsphere positioned at a different distance from the focus point of the camera (see MATERIALS AND METHODS). For our custom-built microscope, across a range of ±10 μm, the values of total flu-

Published August 30, 2004

orescence were found to be within 20% of that when the microsphere was in focus. Similar results were also obtained with the commercially available microscope (Fig. S1, available at http://www.jgp.org/cgi/content/full/jgp.200409066/DC1). Therefore, the independence of total fluorescence measurements with respect to the relative position of the microsphere from the focal plane is not unique to the custom-built high-speed imaging system used in the present study.

The Linear Relationship between ΔF_{total} and ΔCa^{2+}

The relationship between ΔF_{total} and ΔCa^{2+} depends not only on the concentration of fluo-3, but also on other buffers. Moreover, the constituents are not in equilibrium during a channel opening. Nevertheless, we have previously reported from computer simulations with fluo-3 and a fixed buffer (Zou et al., 1999) that ΔF_{total} increases linearly with time during the channel opening (for a constant Ca^{2+} current from 0.1 to at least 3 pA, a reasonable range for single channel Ca^{2+} currents and currents underlying Ca^{2+} sparks). Consistent with this simulation, our experimental results also show a linear relationship between ΔF_{total} and ΔCa^{2+} (for stretch-activated channels in cell-attached patches see Zou et al., 2002).

A similar linear relationship can also be found in the literature for confocal microscopy. Wang et al. (2001) showed data for openings of L-type Ca^{2+} channels in cell-attached patches at the same potential in cardiac cells, and there appears to be a linear relationship between signal mass and total Ca^{2+} influx. Also, the signal mass for oocyte Ca^{2+} puffs and Ca^{2+} blips increases linearly with time, which suggests a linear relationship between signal mass and Ca^{2+} influx assuming a constant Ca^{2+} current underlying these events (Sun et al., 1998). Furthermore, simulations of the events underlying skeletal muscle Ca^{2+} sparks reveal a near linear relationship between signal mass and the amount of Ca^{2+} release with Ca^{2+} currents of different durations, and a near linear rise in the signal mass over time with a constant, though brief, Ca^{2+} current (Chandler et al., 2003). Therefore, a linear relationship, and hence a constant converting factor, between signal mass or ΔF_{total} and ΔCa^{2+} may be more common than might be expected. The actual value of the converting factor would depend on the experimental conditions.

Two implications are provided by the linear relationship between ΔF_{total} and ΔCa^{2+}. First, determining an unknown Ca^{2+} influx using ΔF_{total} requires only the value of the constant converting factor. There would be no need to develop a (nonlinear) calibration curve to relate ΔF_{total} to the underlying ΔCa^{2+}. Second, the signal mass method is demonstrated to be valid over the whole range of ΔCa^{2+}, from near zero to at least the maximum ΔCa^{2+} obtained by the calibration method using the 90 mM Ca^{2+} solution ($\sim 10^6$ Ca ions from Fig. 3).

Obtaining the value for the converting factor between fluorescence events and Ca^{2+} influx is essential for determining the Ca^{2+} currents underlying fluorescence events when the currents cannot be obtained directly. The converting factor can be obtained with a known Ca^{2+} current through nonselective Ca^{2+}-permeable cation channels (like stretch-activated channels or caffeine-activated channels) or with the Ca^{2+} current passing through Ca^{2+}-selective channels.

A possible drawback of using Ca^{2+}-selective channels as well as stretch-activated channels is that recordings are obtained in cell-attached patches. In cardiac cells it appears that membrane deformation during formation of the "omega-like" cell-attached patch may decrease the coupling between the L-type Ca^{2+} channel opening and Ca^{2+} spark generation (Wang et al., 2001). Furthermore, we have noticed a few ms time shift that sometimes occurs when recording the SCCaFT due to an opening of the stretch-activated channel, which may also be due to the geometry of the cell-attached patch.

There are other advantages for using channels like caffeine-activated channels instead of Ca^{2+}-selective channels (Zou et al., 2004). The unitary current for caffeine-activated channels at −80 mV is five times larger than the Ca^{2+} current, making the unitary currents easier to discern. Because there are only a few caffeine-activated channels on the entire cell membrane, each of which has long openings and larger currents, recordings can be obtained in the same whole-cell patch-clamp configuration used to record Ca^{2+} sparks. Moreover, the cytosolic fluo-3 concentration can be approximated to be the pipette fluo-3 concentration with whole-cell recordings, making it possible to estimate the binding capacity of endogenous buffers.

The Buffer Adjustment Factor and Buffer Binding Capacity

The linear relationship between ΔF_{total} and ΔCa^{2+} suggests that k, and therefore f_b, is a constant. Computer simulations similar to those shown in Zou et al. (1999) were performed to explain this observation using parameters reported in the literature for smooth muscles. The simulations involved an endogenous fixed buffer ($\kappa = 115$ [see below], $k_{on} = 100$ $[\mu M \cdot s]^{-1}$, $k_{off} = 100$ s^{-1}) as well as fluo-3 (50 μM, $k_{on} = 80$ $[\mu M \cdot s]^{-1}$, $k_{off} = 90$ s^{-1}, diffusion constant = 2.5×10^{-7} cm^2/s) with a resting Ca^{2+} level of 50 nM. Results from simulations demonstrated that f_b is indeed essentially constant during a channel opening and its value is close to that at equilibrium. This conclusion remains unchanged when the on and off rates of the fixed buffer were changed by at least a factor of two, varying the concentration to keep κ the same.

Using the value of f_b obtained during our experiments, we can estimate the binding capacity of an

Published August 30, 2004

equivalent endogenous buffer, which is a reflection of the change in Ca^{2+} binding to a particular buffer when the Ca^{2+} concentration is changed (Neher and Augustine, 1992). The binding capacity (κ_B) of any buffer (B), at equilibrium with a given Ca^{2+} concentration and for small Ca^{2+} changes, is $\kappa_B = \partial[CaB]/\partial[Ca] = B_T \cdot K_d/([Ca] + K_d)^2$ (here, K_d is the dissociation constant of the buffer, B_T is the total buffer concentration, and [CaB] is the concentration of Ca^{2+}-bound buffer B). In the present study, the binding capacity of fluo-3 (κ_F) was 41 at rest, assuming a total fluo-3 concentration of 50 μM, a K_d of 1.13 μM, and a resting Ca^{2+} level of 50 nM. The fraction of incoming Ca^{2+} bound to fluo-3, equivalent to the reciprocal of our buffer adjustment factor, can be calculated from $\kappa_F/(\kappa_F + \kappa_E + 1)$ (κ_E is the binding capacity of endogenous buffer). Therefore, from $f_b = 3.86$ (25.9% of the Ca^{2+} entered binds to fluo-3) and $\kappa_F = 41$, we obtained the approximate binding capacity of an equivalent endogenous buffer (an aggregate of all other buffers) under whole-cell recording conditions of 115. This value for endogenous buffer binding capacity in toad stomach smooth muscle cells is in agreement with those determined from other smooth muscle preparations (see Daub and Ganitkevich, 2000, and the references therein).

The Fluorescence Factor

We obtained the values of the fluorescence factor (f) for fluo-3 by measuring the fluorescence emission from a known amount of Ca^{2+}-bound fluo-3 contained in glass capillary tubes. Alternatively, it can be obtained by measuring the fluo-3 florescence emission from a volume segment of a cell at rest. ZhuGe et al. (2000) obtained a calibration factor ($f^{-1} = 2.44$ Ca^{2+}-bound fluo-3 molecules per detected photon) in the same cell type using this alternative method. For this measurement it was assumed that the volume segment was a rectangular cube with a uniform thickness of 8 μm, the resting Ca^{2+} concentration was 100 nM, the total fluo-3 concentration inside the cell was equal to that in the pipette (50 μM), and the K_d was 1.1 μM (see Eq. 6). Using the same imaging system, pixel size (333 × 333 nm), and lens (40× oil immersion lens with a NA = 1.3) as used for Ca^{2+} spark measurements, we determined $f = 0.80$ detected photons per Ca^{2+}-bound fluo-3 molecule directly from rectangular glass capillary tubes without the need for the above assumptions (Fig. 4). This value is about twice that obtained by ZhuGe et al. (2000) ($f = 1/2.44 = 0.41$ detected photons per Ca^{2+}-bound fluo-3 molecule). While the difference could come from the cell volume estimate, it could also be due to the estimate for the resting Ca^{2+} concentration. The values for f obtained using both methods would be in very good agreement (within ~3%, see Eq. 6) if an estimate of 50 nM intracellular Ca^{2+} (close to the value obtained by Guerrero et al., 1994b, for toad cells with 1.8 mM extracellular Ca^{2+}, also see Hollingworth et al., 2001, for frog skeletal muscle) was used instead of 100 nM (close to the value obtained by Drummond and Fay, 1996, with 20 mM extracellular Ca^{2+}).

Determining the Ca^{2+} Currents Underlying Ca^{2+} Sparks

An important consequence of our measurements with the caffeine-activated channel is that it leads to an ability to obtain the Ca^{2+} current underlying Ca^{2+} fluorescence events, like Ca^{2+} sparks, where the current cannot be directly measured. We applied our results to Ca^{2+} sparks recorded previously by ZhuGe et al. (2000) who used the same cell preparation we used here.

ZhuGe et al. (2000) employed an averaging technique using the spark-induced spontaneous transient outward current (STOC) to temporally align the Ca^{2+} sparks and then grouped the Ca^{2+} sparks into quartiles according to their total fluorescence increase or signal mass. From the initial rate of rise of the averaged signal mass for each quartile, the underlying mean Ca^{2+} current was estimated to be 0.23, 0.66, 0.66, and 1.31 pA, respectively. These current values were minimum estimates because they were based on the assumption that all of the Ca^{2+} released through ryanodine receptors would bind to fluo-3 (i.e., $f_b = 1$). If our experimentally determined values of f_b (3.86) and also f (0.80) were applied, the current estimates would be increased to 0.45, 1.31, 1.31, and 2.59 pA, respectively. By doing this, we are effectively applying a converting factor of $k = 3.86/0.8 = 4.83$ (instead of $1/0.41 = 2.44$) to the fluorescence measurements of ZhuGe et al. (2000). This accounted for the binding of the released Ca^{2+} to buffers other than fluo-3 and removed the assumptions involved in calculating the fluorescence factor from the cell.

There has been considerable debate as to whether the smallest of the Ca^{2+} sparks is due to the opening of a single receptor/channel or the concerted opening of a number of channels (Cannell and Soeller, 1999; Schneider, 1999; Shirokova et al., 1999; Gonzalez et al., 2000). Kettlun et al. (2003) estimated, based on their results from bilayer studies, that ryanodine receptors from mammalian cardiac cells and amphibian skeletal muscle have a unitary Ca^{2+} current of ~0.5 pA under near physiological conditions (1 mM luminal Ca^{2+}, symmetric 1 mM Mg^{2+} and 150 mM K^+). The Mg^{2+} and K^+ concentrations are similar to those used for studying Ca^{2+} sparks in toad stomach smooth muscle cells (ZhuGe et al., 2000). If the ryanodine receptor conductance properties are also similar, then the Ca^{2+} spark current estimated from the first quartile of signal mass amplitudes (0.45 pA) is possibly due to the opening of a single ryanodine receptor. Larger sparks may be generated by currents of six or more ryanodine receptors, based on the current calculated from the quartile with

Published August 30, 2004

the largest signal mass being about six times that of the smallest quartile. If the toad cell sarcoplasmic reticulum Ca^{2+} concentration is closer to 0.15 mM as measured by ZhuGe et al. (1999), then the unitary Ca^{2+} currents from ryanodine receptors might be smaller. Therefore, an average Ca^{2+} spark in the first quartile might require more ryanodine receptors to open with possibly the current through one ryanodine receptor underlying the smallest detectable Ca^{2+} spark.

Our estimates of the Ca^{2+} currents underlying Ca^{2+} sparks in gastric smooth muscle cells are in the range of the studies of Wang et al. (2001, 2004), who also used a calibration standard. They estimated the Ca^{2+} current underlying Ca^{2+} sparks in cardiac cells from the time course of the rising phase of the fluorescence transients obtained with confocal linescan imaging. The fluorescence associated with Ca^{2+} influx through L-type Ca^{2+} channels (which they called "sparklets") was used as a calibration standard. Their spark currents varied from ~1 to 10 pA. If the fluorescence transients were recorded in focus, they were able to detect a fine structure in the current amplitude distribution corresponding to a unitary spark current of ~1.2 pA, which they attributed to the current due to a single ryanodine receptor.

Estimating the Underlying Unitary Ca^{2+} Current from ΔF_{total} Measurements Alone

Without simultaneous patch-clamp recordings, it is not that straightforward to obtain the unitary Ca^{2+} current from the rate of rise of ΔF_{total} using Eq. 7, even with the assumption that a single channel opening underlies the fluorescence transient. Although Ca^{2+} influx can be determined from the converting factor and ΔF_{total}, it may provide only the average unitary Ca^{2+} current during the transient. This could happen when continuous rapid closings and reopenings of the channel occur and any discontinuities in ΔF_{total} are not detected. In this case, ΔF_{total} will have a slower rate of rise and, therefore, lead to an underestimate of the open channel unitary Ca^{2+} current (Fig. 1 D).

When the transient is a result of openings of more than one channel, it becomes impossible to estimate the unitary Ca^{2+} current even if the openings and closings are synchronized, although it may be possible to estimate the total underlying Ca^{2+} current. Moreover, nonsynchronous openings and closings of the channels may cause ΔF_{total} to deviate from linearity over time. For example, the rate of rise of ΔF_{total} will decrease when some of the open channels close at different times. However, if all the channels opened synchronously (as suggested by the results of Wang et al., 2004), then measuring the initial rate of rise of ΔF_{total} may provide an estimate of the Ca^{2+} current.

Moreover, the rise time of ΔF_{total} is not the best measure of the channel open time because the spatial integration reduces the contribution from the fluorescence obtained from the location of the channel. On the other hand, when in focus, the localized fluorescence change at the channel ($\Delta F/F_0$ or ΔF) is much more sensitive to the kinetics of its opening and closing (Video 1, available at http://www.jgp.org/cgi/content/full/jgp.200409066/DC1). Therefore, the $\Delta F/F_0$ signal can be used as a reference for channel open and closed states (Zou et al., 1999). Even the out-of-focus $\Delta F/F_0$ or ΔF, although not as sensitive to brief closures as those in focus, can provide a good measure of the single channel open duration. As a result, the combined measurements of the in-focus fluorescence at the channel and ΔF_{total} would provide a good means for determining the Ca^{2+} current. When measuring brief fluorescence events (such as Ca^{2+} sparks with the rise time of $\Delta F/F_0$ usually <20 ms), however, a much faster imaging rate is required to determine accurately the channel open time and distinguish brief closures and reopenings. Unfortunately, higher time resolution (e.g., 2-ms exposure times) also engenders a noisier fluorescence signal.

In conclusion, the calibrated signal mass measurement is a valid method for determining Ca^{2+} influx underlying a fluorescence transient using single wavelength dyes such as fluo-3. A wide-field microscope has advantages over a confocal microscope for such measurements because fewer assumptions are required. Once a system is calibrated with a known Ca^{2+} current (i.e., the converting factor is obtained), it can be used to determine the unknown Ca^{2+} influxes or releases underlying various fluorescence transients when ΔF_{total} can be directly measured.

We thank Stephen Baker for help with the statistical analysis; Agustin Guerrero-Hernández, Michael Kirber, and Michael Sanderson for their comments on an earlier version of the manuscript; and Jeff Carmichael, the late Rebecca McKinney, Brian Packard, Paul Tilander, and Yu Yan for their excellent technical assistance. Jeff Carmichael also helped with the PSF measurements for the commercial microscope.

This work was supported by National Institutes of Health grant AR47067.

Olaf S. Andersen served as editor.

Submitted: 31 March 2004
Accepted: 3 August 2004

REFERENCES

Bootman, M., E. Niggli, M. Berridge, and P. Lipp. 1997. Imaging the hierarchical Ca^{2+} signalling system in HeLa cells. *J. Physiol.* 499:307–314.

Burnashev, N. 1998. Calcium permeability of ligand-gated channels. *Cell Calcium.* 24:325–332.

Cannell, M.B., and C. Soeller. 1999. Mechanisms underlying calcium sparks in cardiac muscle. *J. Gen. Physiol.* 113:373–376.

Carrington, W.A., and K.E. Fogarty. 1987. 3D molecular distribution if living cells by deconvolution of optical sectioning using light microscopy. *Proceedings of the Thirteenth Annual Northeast*

Published August 30, 2004

Bioengineering Conference, IEEE, New York. 1:108–110.

Carrington, W.A., R.M. Lynch, E.D. Moore, G. Isenberg, K.E. Fogarty, and F.S. Fay. 1995. Superresolution three-dimensional images of fluorescence in cells with minimal light exposure. *Science.* 268:1483–1487.

Chandler, W.K., S. Hollingworth, and S.M. Baylor. 2003. Simulation of calcium sparks in cut skeletal muscle fibers of the frog. *J. Gen. Physiol.* 121:311–324.

Cheng, H., W.J. Lederer, and M.B. Cannell. 1993. Calcium sparks: elementary events underlying excitation-contraction coupling in heart muscle. *Science.* 262:740–744.

Daub, B., and V. Ganitkevich. 2000. An estimate of rapid cytoplasmic calcium buffering in a single smooth muscle cell. *Cell Calcium.* 27:3–13.

Drummond, R.M., and F.S. Fay. 1996. Mitochondria contribute to Ca^{2+} removal in smooth muscle cells. *Pflugers Arch.* 431:473–482.

Fay, F.S., R. Hoffmann, S. Leclair, and P. Merriam. 1982. Preparation of individual smooth muscle cells from the stomach of *Bufo marinus. Methods Enzymol.* 85:284-292.

Fogarty, K.E., J.F. Kidd, R.A. Tuft, and P. Thorn. 2000. A bimodal pattern of $InsP_3$-evoked elementary Ca^{2+} signals in pancreatic acinar cells. *Biophys. J.* 78:2298–2306.

Gonzalez, A., W.G. Kirsch, N. Shirokova, G. Pizarro, G. Brum, I.N. Pessah, M.D. Stern, H. Cheng, and E. Rios. 2000. Involvement of multiple intracellular release channels in calcium sparks of skeletal muscle. *Proc. Natl. Acad. Sci. USA.* 97:4380–4385.

Grynkiewicz, G., M. Poenie, and R.Y. Tsien. 1985. A new generation of Ca^{2+} indicators with greatly improved fluorescence properties. *J. Biol. Chem.* 260:3440–3450.

Guerrero, A., F.S. Fay, and J.J. Singer. 1994a. Caffeine activates a Ca^{2+}-permeable, nonselective cation channel in smooth muscle cells. *J. Gen. Physiol.* 104:375–394.

Guerrero, A., J.J. Singer, and F.S. Fay. 1994b. Simultaneous measurement of Ca^{2+} release and influx into smooth muscle cells in response to caffeine. A novel approach for calculating the fraction of current carried by calcium. *J. Gen. Physiol.* 104:395–422.

Harkins, A.B., N. Kurebayashi, and S.M. Baylor. 1993. Resting myoplasmic free calcium in frog skeletal muscle fibers estimated with fluo-3. *Biophys. J.* 65:865–881.

Hollingworth, S., J. Peet, W.K. Chandler, and S.M. Baylor. 2001. Calcium sparks in intact skeletal muscle fibers of the frog. *J. Gen. Physiol.* 118:653–678.

Kettlun, C., A. Gonzalez, E. Rios, and M. Fill. 2003. Unitary Ca^{2+} current through mammalian cardiac and amphibian skeletal muscle ryanodine receptor channels under near-physiological ionic conditions. *J. Gen. Physiol.* 122:407–417.

Kirber, M.T., E.F. Etter, K.A. Bellve, L.M. Lifshitz, R.A. Tuft, F.S. Fay, J.V. Walsh, and K.E. Fogarty. 2001. Relationship of Ca^{2+} sparks to STOCs studied with 2D and 3D imaging in feline oesophageal smooth muscle cells. *J. Physiol.* 531:315–327.

Klein, M.G., H. Cheng, L.F. Santana, Y.H. Jiang, W.J. Lederer, and M.F. Schneider. 1996. Two mechanisms of quantized calcium release in skeletal muscle. *Nature.* 379:455–458.

Koizumi, S., M.D. Bootman, L.K. Bobanovic, M.J. Schell, M.J. Berridge, and P. Lipp. 1999. Characterization of elementary Ca^{2+} release signals in NGF-differentiated PC12 cells and hippocampal neurons. *Neuron.* 22:125–137.

Lassignal, N.L., J.J. Singer, and J.V. Walsh Jr. 1986. Multiple neuropeptides exert a direct effect on the same isolated single smooth muscle cell. *Am. J. Physiol.* 250:C792–C798.

Lopez-Lopez, J.R., P.S. Shacklock, C.W. Balke, and W.G. Wier. 1995. Local calcium transients triggered by single L-type calcium channel currents in cardiac cells. *Science.* 268:1042–1045.

Neher, E. 1995. The use of fura-2 for estimating Ca buffers and Ca fluxes. *Neuropharmacology.* 34:1423–1442.

Neher, E., and G.J. Augustine. 1992. Calcium gradients and buffers in bovine chromaffin cells. *J. Physiol.* 450:273–301.

Nelson, M.T., H. Cheng, M. Rubart, L.F. Santana, A.D. Bonev, H.J. Knot, and W.J. Lederer. 1995. Relaxation of arterial smooth muscle by calcium sparks. *Science.* 270:633–637.

Ohyama, T., D.H. Hackos, S. Frings, V. Hagen, U.B. Kaupp, and J.I. Korenbrot. 2000. Fraction of the dark current carried by Ca^{2+} through cGMP-gated ion channels of intact rod and cone photoreceptors. *J. Gen. Physiol.* 116:735–754.

Parker, I., and Y. Yao. 1991. Regenerative release of calcium from functionally discrete subcellular stores by inositol trisphosphate. *Proc. R. Soc. Lond. B. Biol. Sci.* 246:269–274.

Rios, E., and G. Brum. 2002. Ca^{2+} release flux underlying Ca^{2+} transients and Ca^{2+} sparks in skeletal muscle. *Front. Biosci.* 7: d1195–d1211.

Rios, E., M.D. Stern, A. Gonzalez, G. Pizarro, and N. Shirokova. 1999. Calcium release flux underlying Ca^{2+} sparks of frog skeletal muscle. *J. Gen. Physiol.* 114:31–48.

Schneider, M.F. 1999. Ca^{2+} sparks in frog skeletal muscle: generation by one, some, or many SR Ca^{2+} release channels? *J. Gen. Physiol.* 113:365–372.

Shen, J.X., S. Wang, L.S. Song, T. Han, and H. Cheng. 2004. Polymorphism of Ca^{2+} sparks evoked from in-focus Ca^{2+} release units in cardiac myocytes. *Biophys. J.* 86:182–190.

Shirokova, N., A. Gonzalez, W.G. Kirsch, E. Rios, G. Pizarro, M.D. Stern, and H. Cheng. 1999. Calcium sparks: release packets of uncertain origin and fundamental role. *J. Gen. Physiol.* 113:377–384.

Smith, G.D., J.E. Keizer, M.D. Stern, W.J. Lederer, and H. Cheng. 1998. A simple numerical model of calcium spark formation and detection in cardiac myocytes. *Biophys. J.* 75:15–32.

Sun, X.P., N. Callamaras, J.S. Marchant, and I. Parker. 1998. A continuum of $InsP_3$-mediated elementary Ca^{2+} signalling events in *Xenopus* oocytes. *J. Physiol.* 509:67–80.

Wang, S.Q., L.S. Song, E.G. Lakatta, and H. Cheng. 2001. Ca^{2+} signalling between single L-type Ca^{2+} channels and ryanodine receptors in heart cells. *Nature.* 410:592–596.

Wang, S.Q., M.D. Stern, E. Rios, and H. Cheng. 2004. The quantal nature of Ca^{2+} sparks and in situ operation of the ryanodine receptor array in cardiac cells. *Proc. Natl. Acad. Sci. USA.* 101:3979–3984.

Wellman, G.C., and M.T. Nelson. 2003. Signaling between SR and plasmalemma in smooth muscle: sparks and the activation of Ca^{2+}-sensitive ion channels. *Cell Calcium.* 34:211–229.

Zhou, J., G. Brum, A. Gonzalez, B.S. Launikonis, M.D. Stern, and E. Rios. 2003. Ca^{2+} sparks and embers of mammalian muscle. Properties of the sources. *J. Gen. Physiol.* 122:95–114.

ZhuGe, R., K.E. Fogarty, R.A. Tuft, L.M. Lifshitz, K. Sayar, and J.V. Walsh Jr. 2000. Dynamics of signaling between Ca^{2+} sparks and Ca^{2+}- activated K^+ channels studied with a novel image-based method for direct intracellular measurement of ryanodine receptor Ca^{2+} current. *J. Gen. Physiol.* 116:845–864.

ZhuGe, R., R.A. Tuft, K.E. Fogarty, K. Bellve, F.S. Fay, and J.V. Walsh Jr. 1999. The influence of sarcoplasmic reticulum Ca^{2+} concentration on Ca^{2+} sparks and spontaneous transient outward currents in single smooth muscle cells. *J. Gen. Physiol.* 113:215–228.

Zou, H., L.M. Lifshitz, R.A. Tuft, K.E. Fogarty, and J.J. Singer. 1999. Imaging Ca^{2+} entering the cytoplasm through a single opening of a plasma membrane cation channel. *J. Gen. Physiol.* 114:575–588. (published erratum appears in *J. Gen. Physiol.* 1999. 114:839)

Zou, H., L.M. Lifshitz, R.A. Tuft, K.E. Fogarty, and J.J. Singer. 2002. Visualization of Ca^{2+} entry through single stretch-activated cation channels. *Proc. Natl. Acad. Sci. USA.* 99:6404–6409.

Zou, H., L.M. Lifshitz, R.A. Tuft, K.E. Fogarty, and J.J. Singer. 2004. Imaging calcium entering the cytosol through a single opening of plasma membrane ion channels: SCCaFTs - fundamental calcium events. *Cell Calcium.* 35:523–533.